



# Microtribological properties of molecularly thin carboxylic acid functionalized imidazolium ionic liquid film on single-crystal silicon

Yufei Mo<sup>a,b</sup>, Bo Yu<sup>a</sup>, Wenjie Zhao<sup>a,b</sup>, Mingwu Bai<sup>a,\*</sup>

<sup>a</sup> State Key Laboratory of Solid Lubrication, Lanzhou Institute of Chemical Physics, Chinese Academy of Sciences, Lanzhou 730000, China

<sup>b</sup> Graduate School of Chinese Academy of Sciences, Beijing 100039, China

## ARTICLE INFO

### Article history:

Received 11 March 2008

Received in revised form 3 July 2008

Accepted 11 July 2008

Available online 22 July 2008

### Keywords:

Ionic liquid

Bonding percentage

Tribology

MEMS

## ABSTRACT

A series of 1-alkyl-3-ethylcarboxylic acid imidazolium chloride ([AEImi][Cl]) ionic liquids was synthesized and evaluated as a new kind of lubricant for microelectromechanical system (MEMS). In this research, novel molecular thin ionic liquid films (ILs) with various bonding percentages were prepared with different annealing temperatures and times. Film wettability was determined by measurement of contact angle and thickness with the ellipsometric method. The chemical composition, structure and morphology were characterized by the means of multi-technique X-ray photoelectron spectrometric, and atomic force microscopic analysis, respectively. The nano- and microtribological properties of the ionic liquid film were investigated. The morphologies of wear tracks of IL films were examined using a 3D non-contact profilometer. The influence of chain length on friction in nano-scale, and the effect of bonding percentage and sliding frequency on friction coefficient, carry-bearing capacity and durability in micro-scale were studied. Data are compared to the perfluoropolyether lubricant Z Dol. The [AEImi][Cl] ionic liquid films with appropriate bonding percentage exhibited comparable load-bearing capacity and durability than Z Dol 3800 at thickness level of several nanometers. Therefore, the [AEImi][Cl] ionic liquid film shows strong potential applications involving the lubrication and protection of MEMS.

© 2008 Elsevier B.V. All rights reserved.

## 1. Introduction

Perfluoropolyethers (PFPEs), e.g. Z Dol, have very low vapor pressure and good stability at high temperature. Z Dol film can presently be coated as thin as 1–2 nm and is utilized as lubricants in rigid magnetic disks, precision instruments and MEMS in order to minimize friction, wear and contamination [1]. However, PFPEs are often subjected to degradation catalyzed by strong nucleophilic agents and strong electropositive metals [2,3], which together with the high cost of PFPEs can limit their applications in some fields. Thus, it is necessary to find alternatives for PFPEs [4].

Room temperature ionic liquids (RTILs), which are made of weakly bond anions and usually large organic cations, are a special class of salts having a melting point below room temperature. These fluids are currently being employed as green solvents for a wide range of applications in synthesis, catalysis, electrochemistry, and liquid–liquid extractions [5–9]. As pointed out by Ye et al. [10], RTILs are promising versatile lubricants for many frictional pairs such as

steel/steel, steel/aluminum, steel/copper, steel/silicon steel/sialon ceramics in the macro-scale [11,12]. RTILs exhibit not only excellent friction reduction and anti-wear properties, but also low vapor pressure, non-flammability and high thermal stability [13]. However, so far only few reports have investigated the tribological behavior of molecular thin films of various RTILs, which is critical for their application in MEMS, similar to their applications as lubrication additives and lubricants in the macro-scale [14–17].

Over the past years, many molecular thin films have been studied, such as fatty acids, silanes, thiols, phospholipids, and polymeric films [18–20]. These films can provide load supporting strength owing to high packing density and solid-state-like properties. However, these monolayer films did not last long under repeated sliding. When some of molecules are removed from the surface by mechanical rubbing, the films tend to fracture and break down. To meet this dual requirement, one way is to employ a mixed molecular system where one species will bind to the surface and another species will be allowed to move freely on the surface [21].

Silicon has been widely used as MEMS material. High thermal conductivity, large break down field, and high saturation velocity makes it an ideal choice for high temperature, high power, and high voltage electronic devices. In addition, its physicochemical

\* Corresponding author. Tel.: +86 931 4968080; fax: +86 931 4968080.  
E-mail address: [mwbai@LZB.ac.cn](mailto:mwbai@LZB.ac.cn) (M. Bai).

stability, high melting temperature, extreme hardness make silicon as an attractive material for fabricating sensors and actuators that are capable of performing in harsh environments, such as high temperature, and corrosive and abrasive media. However, from a tribological point of view, friction reduction, wear resistance and durability of this material can be further improved [22].

In this work, we designed carefully ionic liquid molecules assembly exhibiting good mobility and strong chemical bonding at a monolayer level. This strategy leads to the best combination of tribological properties of RTILs, especially for lubrication, friction control and wear protection of MEMS.

## 2. Experimental

### 2.1. Materials

Polished and cleaned single-crystal silicon (100) wafers, obtained from GRINM Semiconductor Materials Co., Ltd. Beijing, were used as substrates for all the data presented in this work. PFPE (formula  $\text{HOCH}_2\text{CF}_2\text{O}-(\text{CF}_2-\text{CF}_2\text{O})_m-(\text{CF}_2\text{O})_n-\text{CF}_2\text{CH}_2\text{OH}$ ,  $m$  and  $n$  are integers, MW 3800, with the commercial name Z Dol 3800) and HFE 7100 were purchased from Aldrich Chem. Co. and used as received. A series of 1-alkyl-3-ethylcarboxylic acid imidazolium chloride,  $[\text{C}_n\text{H}_{2n+1}[\text{CH}_2\text{COOH}]\text{Im}]\text{Cl}$  ionic liquids (denoted as  $\text{C}_n[\text{AEI-mi}][\text{Cl}]$ ,  $n = 1, 4, 8$ ) were synthesized according to reported methods and procedures [23]. Their chemical structures are as follows:

### 2.2. Pretreatment of silicon wafers

Silicon wafers were cleaned and hydroxylated by immersing them in piranha solution (a mixture of 7:3 (v/v) 98%  $\text{H}_2\text{SO}_4$  and 30%  $\text{H}_2\text{O}_2$ ) at 90 °C for 30 min to get a hydroxyl-terminated surface. The modified Si substrates were rinsed with chloroform, isopropanol, ethanol, and acetone in turn to remove the other physisorbed ions and molecules. The substrates were then dried with a nitrogen flow.

### 2.3. Film preparation

The solution of  $[\text{AEI-mi}][\text{Cl}]$  ionic liquid in ethanol with a concentration of 0.02% (w/v) was dip-coated onto the pretreated silicon substrates at a velocity of 60  $\mu\text{m/s}$ , and dried in air for 1 h.

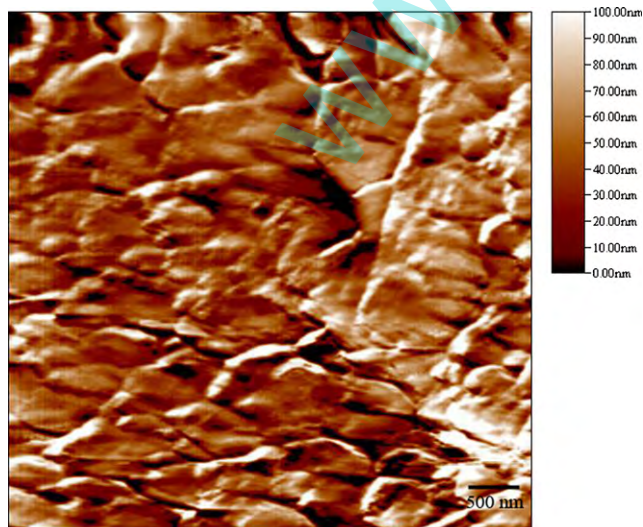


Fig. 1. AFM topography of the steel ball surface.

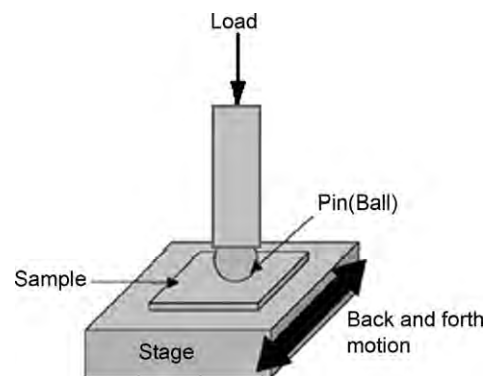


Fig. 2. Schematic illustration of pin-on-plate tribometer.

The thicknesses of the films after dip coating were measured as 1 nm by the ellipsometric method. The PFPE films were prepared from a solution of 0.03% (w/v) Z Dol 3800 in HFE 7100 in the same manner, and were also determined to be 1 nm thick. All procedures were carried out in a class-10 clean room at a humidity of 15% RH and temperature of 20 °C.

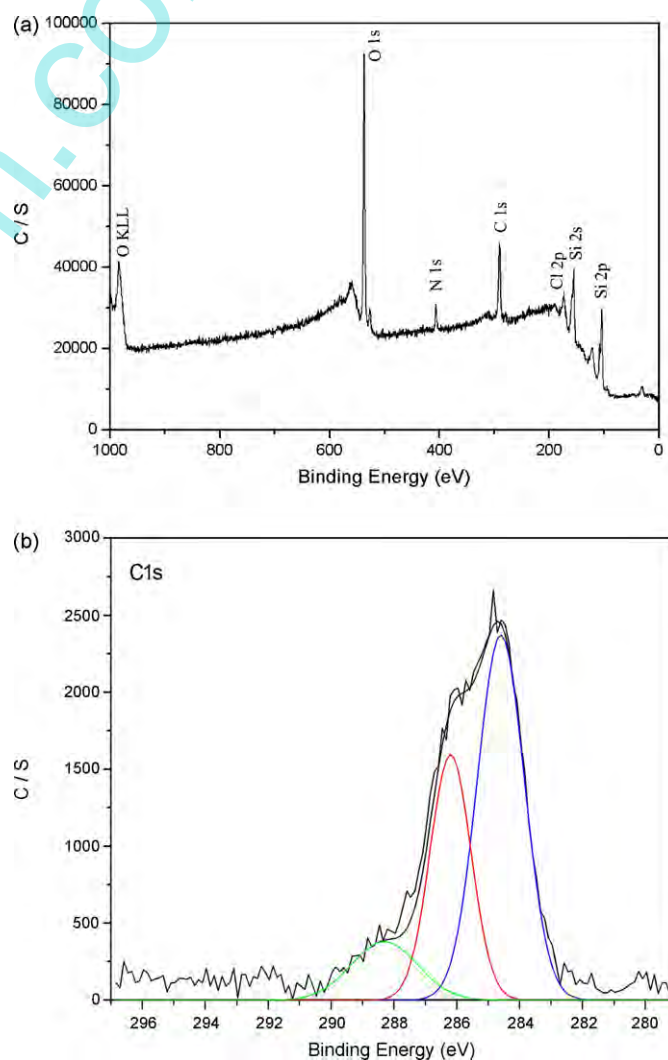


Fig. 3. XPS spectra of  $[\text{AEI-mi}][\text{Cl}]$  ionic liquid-coated silicon surface: (a) survey and (b) C1s spectrum.

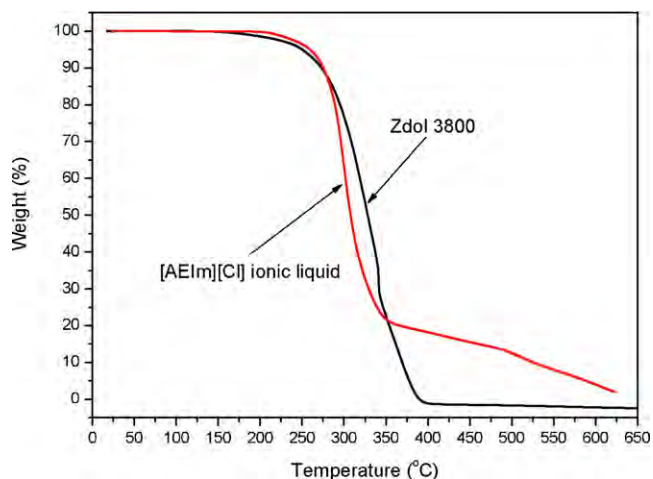


Fig. 4. TGA curve of [AEIm][Cl] ionic liquid.

#### 2.4. Characterization of film

The static contact angles for ultra-pure water on the films were measured with a commercial CA-A type contact-angle measurement apparatus (Kyowa Scientific Co. Ltd). At least five measurements were made for each specimen and the measurement error was below  $2^\circ$  in each case.

The thickness of the films was measured on a Gaertner L116-E ellipsometer, which was equipped with a He-Ne laser (632.8 nm) set at an incident angle of  $50^\circ$ . A real reflective index of 1.46 was set for the silica layer and 1.30 for organic films. The data were collected from 10 different positions for each specimen to get the averages.

Chemical composition and structure of the surface were examined with a PHI-5702 multi-technique X-ray photoelectron spectrometer (XPS), using a pass energy of 29.35 eV, an excitation source of Mg  $K\alpha$  radiation ( $h\nu = 1253.6$  eV) and take-off angle of  $36^\circ$ . The chamber pressure was about  $3 \times 10^{-8}$  Torr during testing. Peak deconvolution of elements was accomplished using the software and sensitivity factors supplied by the manufacturer. The binding energy of adventitious carbon (C1s: 284.8 eV) was used as a reference.

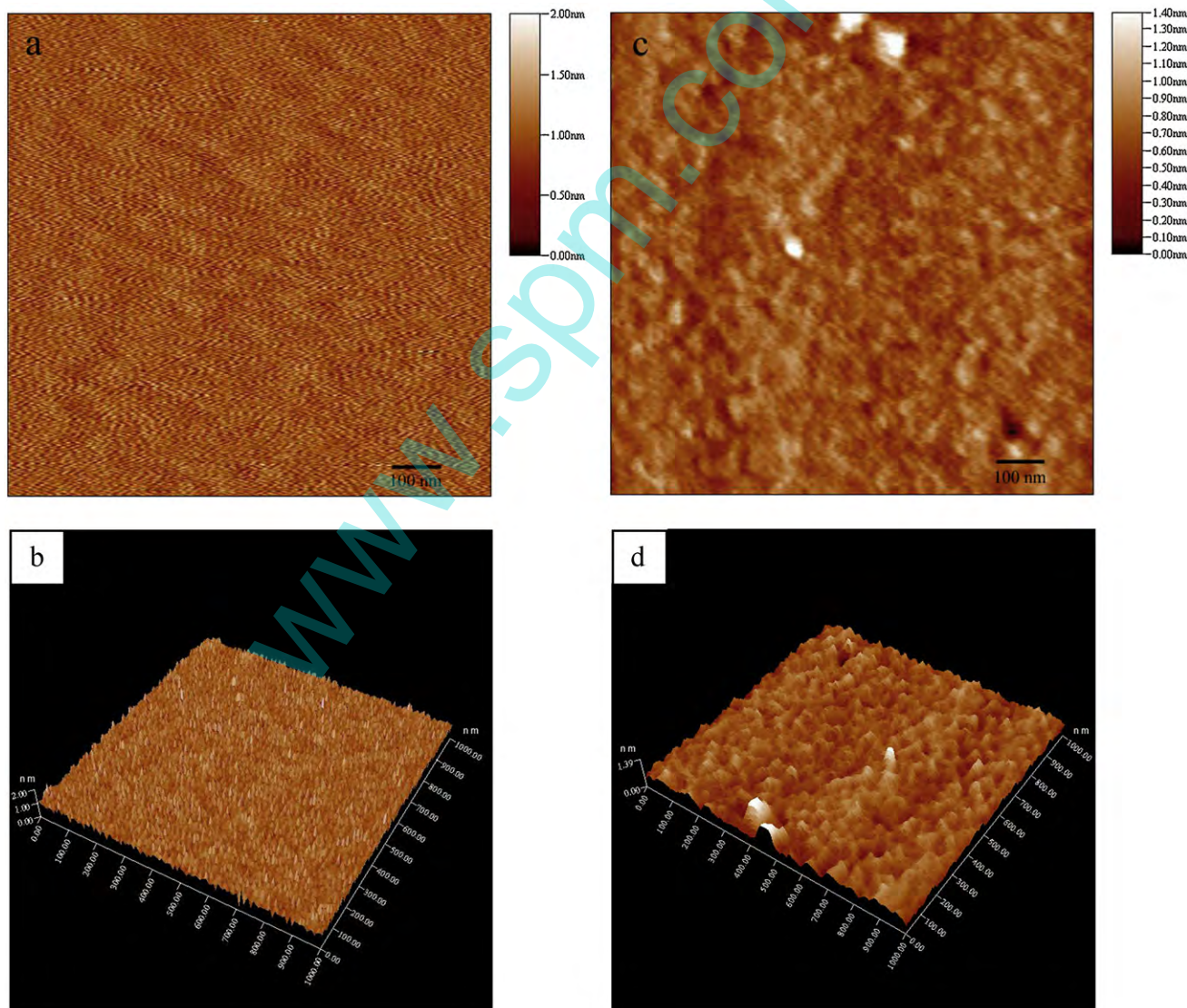


Fig. 5. 2D and 3D AFM images for bare Si wafer before (a and b) and after (c and d) dip-coating treatment in the [AEIm][Cl] ionic liquid solution.

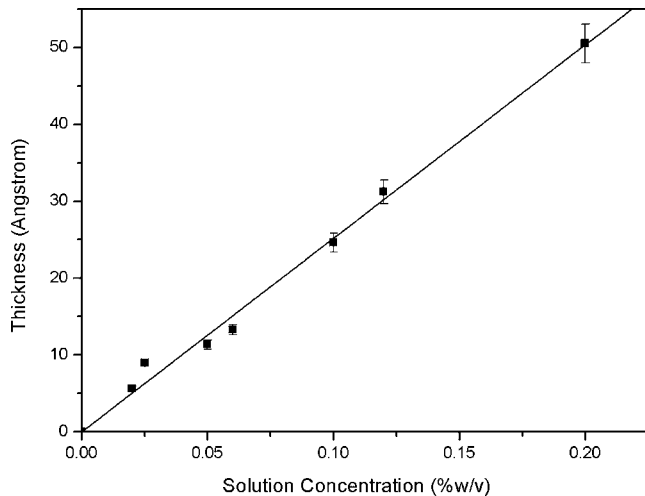


Fig. 6. Plots of film thickness as function of [AEImi][Cl] ionic liquid solution concentration at a pull-off velocity of 60  $\mu\text{m/s}$ .

### 2.5. Nano-friction measurement

The nanotribological behaviors of the films were characterized with an AFM/FFM controlled by CSPM4000 electronics, using the contact mode. Commercially available rectangle  $\text{Si}_3\text{N}_4$  cantilevers with a normal force constant, 0.4 N/m, a radius of less than 10 nm and backside coated by gold (Budgetsensors Instruments Inc.) were employed. The friction force is a lateral force exerted on a tip during scanning and can be measured using the twist of the tip/cantilever assembly. To obtain friction data, the tip was scanned back and forth in the x direction in contact with sample at a constant load while the lateral deflection of the lever was measured. The differences in the lateral deflection or friction signal between back and forth motions are proportional to the friction force. Friction forces were continuously measured with various external loads. The load was increased (or decreased) linearly in each successive scan line and normal loads ranged from 5 to 130 nN. Scanning for the friction force measurement was performed at rate of 1 Hz along the scan axis and a scan size of  $1 \mu\text{m} \times 1 \mu\text{m}$ . The scan axis was perpendicular to the longitudinal direction of the cantilever. The sets of data were displayed graphically in a friction image.

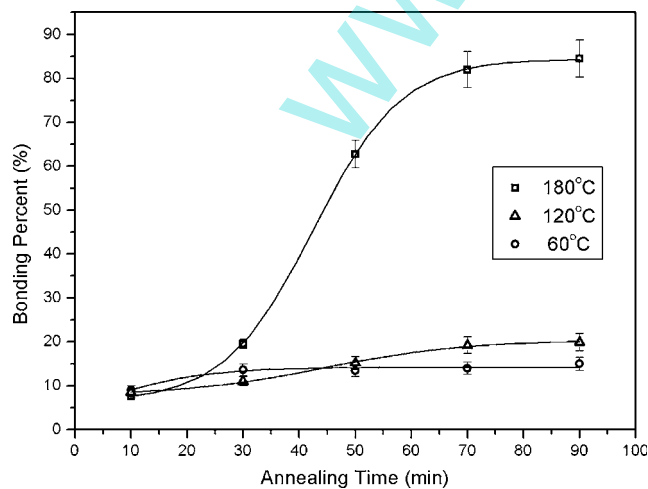


Fig. 7. Bonding percentage as function of annealing time for the [AEImi][Cl] ionic liquid film.

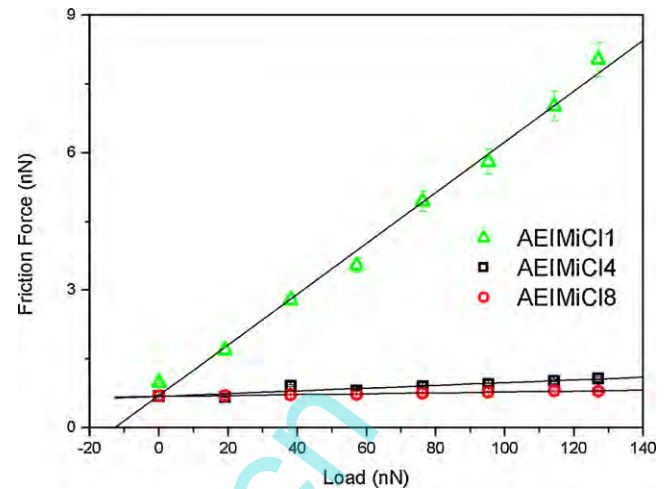


Fig. 8. Plots of friction force versus applied loads for [AEImi][Cl] IL monolayer films with various chain lengths.

### 2.6. Micro-friction and wear test

The friction and wear properties of all these films were evaluated using a UMT-2MT tribometer operating in the reciprocating mode. A standard AISI-52100 steel ball of 3.18 mm in diameter was selected as the counterpart. Fig. 1 shows the surface topography of a ball. The root-mean-square (RMS) roughness of the ball was estimated to be about 24 nm by using AFM. After ultrasonicated in acetone, the ball was fixed in a stationary holder sustained by a beam and the samples were then mounted on a reciprocating table. The ball moved horizontally with respect to the sample surface with a sliding frequency between 1 and 6 Hz and a traveling distance of 5 mm. Applied normal loads used were between 60 and 500 mN and the change in the friction coefficient was monitored versus sliding time or cycles. The initiation of wear on the sample surface leads to an increase in the friction coefficient, and a sharp increase was interpreted to indicate film failure. The friction coefficient and sliding times were recorded automatically by a computer, and at least three repeated measurements were performed. A schematic illustration of the tribometer is shown in Fig. 2. All the tests were conducted at room temperature and at a relative humidity of 45%.

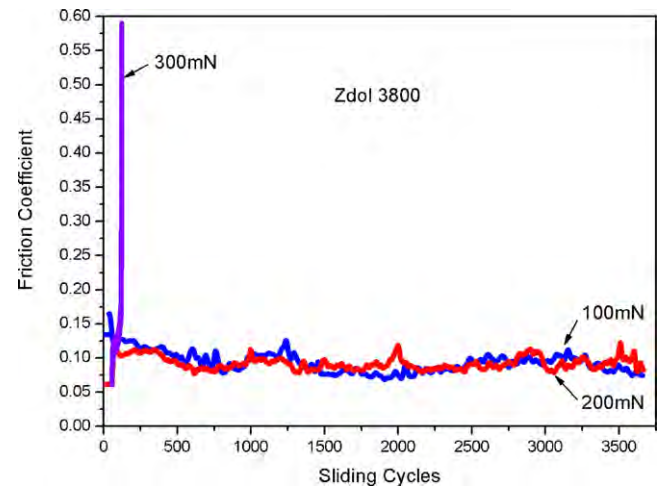
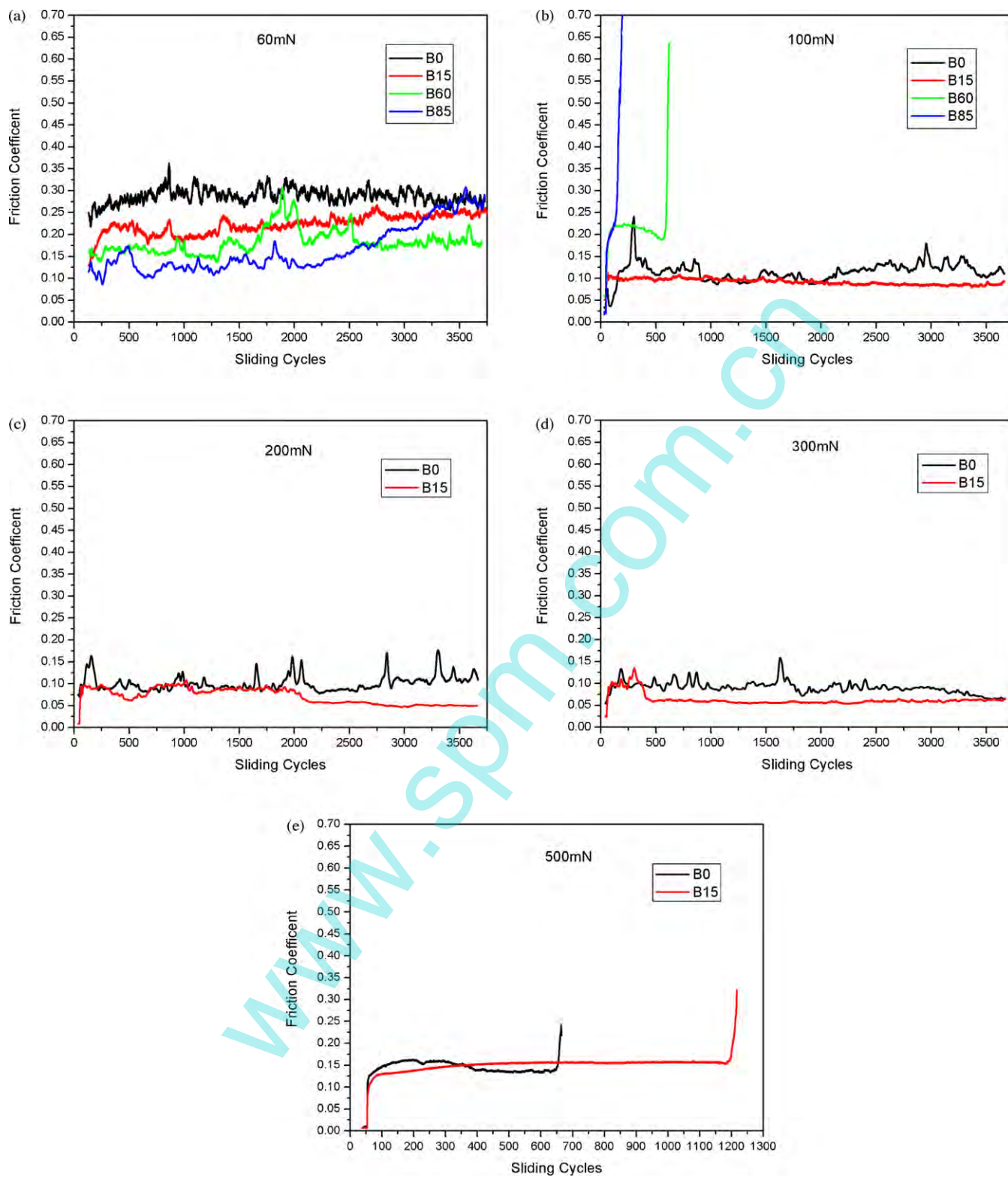


Fig. 9. Plots of friction coefficients versus sliding cycles for Z Dol 3800 film on silicon.



**Fig. 10.** Plots of friction coefficient of [AEIm][Cl] ionic liquid films with various bonding percentages as function of sliding cycles against steel ball at normal loads of (a) 60 mN, (b) 100 mN, (c) 200 mN, (d) 300 mN, (e) 500 mN with a sliding velocity of 10 mm/s. (The films bonding percentages of 0%, 15%, 60%, and 85% were denoted as B0, B15, B60, and B85, respectively.)

**Table 1**

Contact angles and thicknesses for modified silicon, Z Dol 3800 and [AEImi][Cl] ionic liquid film surfaces

Test samples	Water contact angle (°)	Thickness (nm)
SiO <sub>2</sub> /Si	<5	1.8
Z Dol 3800 film	105	~1.0
[AEImi][Cl] ionic liquid film	64	~1.0

### 3. Results and discussion

#### 3.1. Characterization of ionic liquid and films

Measuring contact angle is an effective way to reveal the variation of solid surface chemical composition, especially its wettability. The contact angles of water on the hydroxylated silicon surface, Z Dol 3800 and [AEImi][Cl] ionic liquid film (IL) surfaces are listed in Table 1. The hydroxylated silicon surface was hydrophilic and the contact angle was below 5°. The measured contact angles of the Z Dol 3800 and [AEImi][Cl] ionic liquid on silicon surfaces were about 105° and 64°, respectively. Fig. 3a shows the XPS survey spectrum of [AEImi][Cl] ionic liquid-coated silicon surface. The scan survey spectrum of the film surface shows five elements: carbon (C1s), oxygen (O1s), silicon (Si2p), nitrogen (N1s) and chlorine (Cl2p). As shown in Fig. 3b, there are three peaks arising from C1s XPS spectrum. The first peak at 284.6 eV is assigned to the CH<sub>2</sub> group in [AEImi][Cl], while the second peak at 286.4 eV might originate from the C atoms bonded to the N atoms (C<sup>+</sup>-N) [24]. The third peak at 288.3 eV can be attributed to the carboxyl C atom (O-C<sup>+</sup>=O) [24]. The results indicate that [AEImi][Cl] ionic liquid was successfully coated on the silicon surface.

The thermal stability of [AEImi][Cl] ionic liquid and Z Dol 3800 were examined by thermogravimetric analysis (TGA) between 20 and 600 °C. As shown in Fig. 4, [AEImi][Cl] ionic liquid possess a high decomposition temperature and low vapor loss. There is little weight loss below 250 °C almost the same as Z Dol 3800.

Fig. 5a–d shows 2D and 3D AFM images for the bare Si wafer before and after dip-coating treatment in the [AEImi][Cl] ionic liquid solution. Fig. 5a and b shows that the bare Si wafer surface is smooth and uniform with a root-mean-square (RMS) roughness of about 0.18 nm. The 2D and 3D surface topographies of the [AEImi][Cl] ionic liquid film, as shown in Fig. 5c and d, indicate that the film was homogeneously distributed on the silicon surface with the RMS roughness of about 0.12 nm.

#### 3.2. Film thickness and bonding percentage

Fig. 6 shows the plots of film thickness as function of [AEImi][Cl] ionic liquid solution concentration. The data indicates that the linear increase in film thickness is associated with increase of the solution concentration. According to this relationship, a desired thickness of film was easily prepared. In our research, the lubricant adsorbed onto silicon after the solvent rinsing process, which is termed as bonding lubricant. The bonding percentages of ionic liquid were measured in term of the thickness of ionic liquid adsorbed onto silicon surface (%bonding = 100 × final film thickness/initial film thickness). Sinha et al. gave a definition [25]. Fig. 7 shows the influence of annealing time on bonding percentages with various heating temperature. The data presented are just for after coating and annealing of ionic liquid on silicon with different heating temperature. It can be seen that the ionic liquid was prone to bond with silicon at heating temperature up to 180 °C. It is observed that bonding percentages

increases with annealing time and then tends to stabilize at some constant value.

#### 3.3. AFM nano-friction behavior and chain length effect

The relationship between friction force and external loads for [AEImi][Cl] ionic liquid with various alkyl chain lengths (viz. C1, C4, C8) is shown in Fig. 8. In general, friction is reduced with increase of chain length, and the C<sub>8</sub>[AEImi][Cl] ionic liquid exhibits lowest friction force compared to the others. In the formation of the bonding coatings, both the surface energy and inter-chain interactions play important roles and determine quality of the films [26]. Since the [AEImi][Cl] ionic liquid with same terminal group, the nano-friction property is determined by inter-chain interactions.

#### 3.4. Micro-friction measurements and bonding percentage effect

To understand the influence of the ratio of bonding to the mobile section on the friction in micro-scale behavior, the mixed IL films were compared with different ratios of bonding to mobile section to understand the effect of different bonding percentages. In the test, the four kinds of samples (viz. 0%, 15%, 60% and 85% denoted as B0, B15, B60, and B85) were prepared by controlling annealing temperatures and times.

Fig. 9 shows friction coefficients as function of sliding cycles for Z Dol 3800 on silicon substrates at various loads. The Z Dol 3800 film on hydroxylated silicon showed better tribological performance than silicon with other pretreatment [27]; thus, Z Dol 3800 film on hydroxylated silicon was chosen as reference for comparing the performance of the various IL films. As shown in Fig. 9, the Z Dol 3800 films exhibited an extended durability of 3600 cycles below 200 mN. When the load rose to 300 mN, the Z Dol 3800 films failed upon reaching at 50 sliding cycles.

Fig. 10a–e shows the friction coefficients and sliding cycles of [AEImi][Cl] ionic liquid with various bonding percentages, as function of sliding cycles against a steel ball at normal loads ranging between 60 and 500 mN and a sliding velocity of 10 mm/s. Fig. 10a shows the IL films bonding percentage of 0%, 15%, 60%, and 85% at normal load of 60 mN, an average friction coefficient of 0.28, 0.22, 0.18, and 0.16 was recorded, respectively. It was observed that the films with higher bonding percentage exhibited a lower friction coefficient.

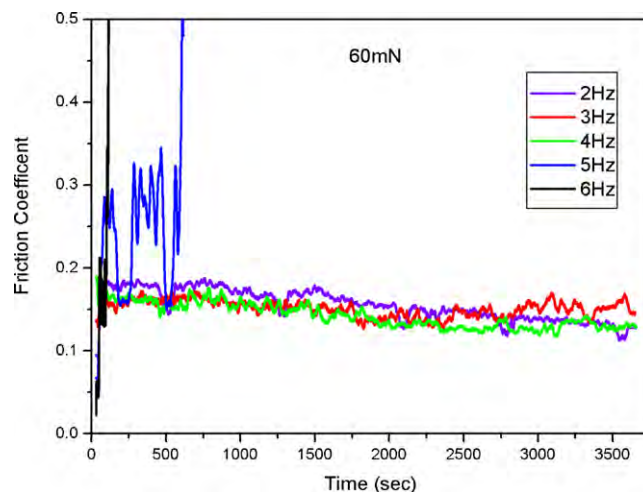
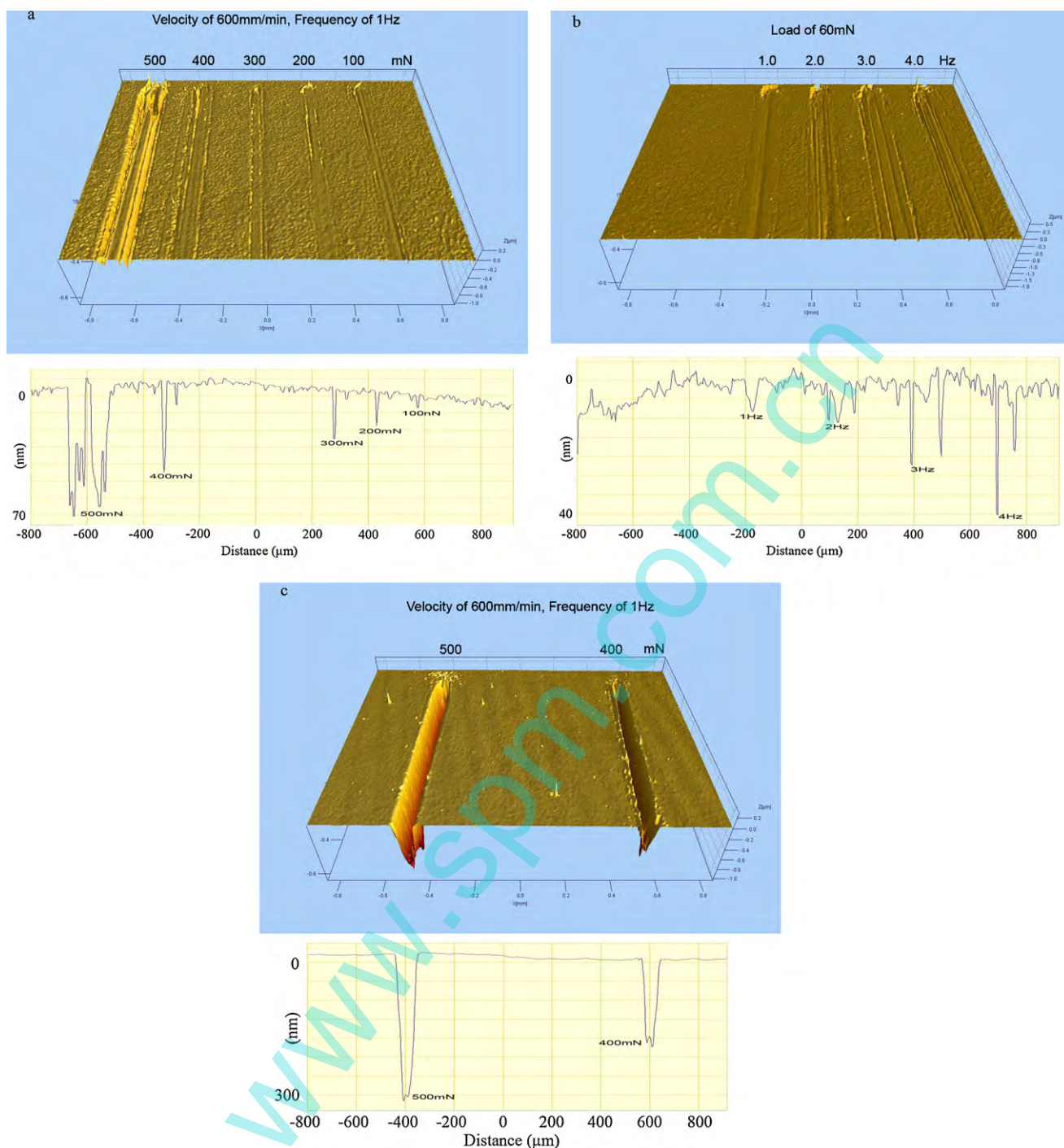


Fig. 11. Plots of coefficient of friction as function of sliding frequency for IL film without annealing at a normal load of 60 mN.



**Fig. 12.** 3D non-contact profilometer images and 2D profiles of the worn surfaces of [AEIm][Cl] ionic liquid and Z Dol 3800 films after sliding against a steel ball for 3600 cycles. (a) 3D image and cross section map of scratch of the IL film at various load and a frequency of 1 Hz (viz. velocity of 600 mm/min). (b) 3D image and cross section map of scratch of the IL film at 60 mN and at various frequencies. (c) 3D image and cross section map of scratch of Z Dol 3800 film at various loads and a frequency of 1 Hz.

As shown in Fig. 10b, when the normal load rose to 100 mN, the friction coefficients of IL bonding percentages of 60% and 85% rose sharply over 0.6 before reaching 450 and 100 cycles, respectively. This value of the friction coefficient is the same as in the case of bare silicon sliding against steel ball counterpart, and this indicates that these films failed completely under the given test conditions. At the same time, the friction coefficients of IL bonding percentages of 0% and 15% were still stable and showed a low value under all sliding cycles, even at load of 200 and 300 mN, as shown in Fig. 10c and d.

When the normal load rose to 500 mN, the IL bonding percentages of 0% and 15% friction coefficients abruptly increased at 600 and 1200 cycles, respectively, as shown in Fig. 10e. This result indicates that wear of the substrate surface occurred and these films failed.

Fig. 11 shows the effect of sliding frequency on coefficient of friction for IL film without annealing at normal load of 60 mN. The friction coefficient of IL was almost stable and low below a sliding frequency of 4 Hz. When the sliding frequency rose over 4 Hz, the friction coefficient value of IL films sharply increased over 0.6 in

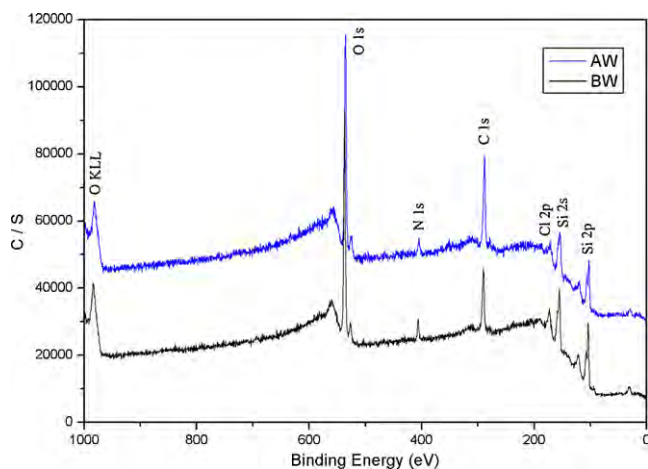


**Fig. 13.** The XPS survey spectra of the IL films on silicon surface before and after wear test (BW: before wear test; AW: after wear test).

several minutes, indicating that the IL films failed completely under higher frequent reciprocating movement.

To further clarify the friction behavior, the worn surfaces 3D and cross-section 2D maps were examined, as shown in Fig. 12a–c. Fig. 12a shows the worn surface of the IL film at various loads and a frequency of 1 Hz (viz. velocity of 10 mm/s) after sliding against the steel ball for 3600 cycles. Fig. 12b shows the morphologies of the worn surface of the IL film at 60 mN and at various frequencies after sliding against the steel ball for 3600 s. The IL film exhibited slighter wear than Z Dol 3800 (Fig. 12c) under the same test conditions. As shown in Fig. 12a and b, there are existed obvious evidences of IL liquid flowing back into the wear tracks. It is observed that some regions of the wear tracks were filled with lubricant, especially at lower load and frequencies. This result indicates that the IL had good mobility on silicon surface.

Fig. 13 shows the XPS survey spectra of IL films on silicon surface before and after wear test. No obvious chemical shift was observed after sliding tests, indicating that there was no chemical change occurred during the friction process and the good tribological performance of the IL film was not caused by producing of new chemical component.

From these results, it could be observed that the IL films with lower bonding percentages, such as 15%, exhibited lower friction coefficient and longer durability and load-bearing capacity than higher bonding percentages and untreated films in the test range of the load. This indicates that the bonding layer can provide load supporting with high strength capabilities while adsorbing onto the silicon surface. From observing the worn surfaces, we can find some evidence of ionic liquid flowing back into the wear tracks of the film. This result indicates that the mobility of the IL molecules can reorganize themselves into the original state after being mechanically disrupted under sliding, namely, the IL mobile layer has a self-repairing property. In addition, the viscoelastic layer between sliding pair acts as a shock absorber to reduce the amount of impact energy transferred to the substrate, which may allow for wear protection under higher frequent reciprocating movement.

#### 4. Conclusions

This study has demonstrated that novel molecularly thin carboxylic acid functionalized imidazolium films could be prepared on single-crystal silicon surface. The tribological properties of the [AEImi][Cl] ionic liquid films were studied. On the basis of the results described above, we can conclude the following:

- (1) [AEImi][Cl] ionic liquids with one nanometer thickness was coated and homogeneously distributed on hydroxylated silicon surface.
- (2) The [AEImi][Cl] ionic liquids have comparable thermal stability, friction coefficient, load-bearing capability, and durability with the commercial lubricant Z Dol.
- (3) All [AEImi][Cl] ionic liquid films exhibit stable and low friction coefficient at mild conditions of 60 mN and 1–4 Hz.
- (4) [AEImi][Cl] ionic liquid film with appropriate bonding percentages, such as 15%, exhibits highest load-bearing capacity and longest durability.

From a tribological point of view, the [AEImi][Cl] ionic liquid shows strong potential as lubricant for MEMS because they have desirable thermal and tribological properties.

#### Acknowledgment

This work was funded by Innovative Group Foundation from National Natural Science Foundation of China (NSFC) under Grant Number 50421502, National 973 Program: 2007CB607601, NSFC 50675217, and “100 Talents” Program of Chinese Academy of Sciences.

#### References

- [1] A. Khurshudov, R.J. Waltman, *Wear* 251 (2001) 1124.
- [2] G. Caporiccio, L. Flabbi, G. Marchionniand, G.T. Viola, *J. Synth. Lubr.* 6 (1989) 133.
- [3] S. Mori, W. Morales, *Wear* 132 (1989) 111.
- [4] W.M. Liu, F. Zhou, L. Yu, G.M. Chen, B. Li, G.H. Zhao, *J. Mater. Res.* 17 (2002) 2357.
- [5] T. Welton, *Chem. Rev.* 9 (2005) 2071.
- [6] P. Wasserscheid, W. Keim, *Angew. Chem. Int. Ed.* 39 (2000) 3772.
- [7] J.G. Huddleston, A.E. Visser, W.M. Reichert, H.D. Willauer, G.A. Broker, R.D. Roger, *Green Chem.* 3 (2001) 156.
- [8] J. Dupont, R.F. Souza, P.A.Z. Suarez, *Chem. Rev.* 102 (2002) 3667.
- [9] R.D. Roger, K.R. Seddon, *Ionic Liquids: Industrial Applications for Green Chemistry*, ACS Symposium Series 818, American Chemical Society, Washington, DC, 2002.
- [10] C.F. Ye, W.M. Liu, Y.X. Chen, L.G. Yu, *Chem. Commun.* 1 (2001) 2244.
- [11] X. Liu, F. Zhou, Y.M. Liang, W.M. Liu, *Tribol. Lett.* 23 (2006) 191.
- [12] Y.Q. Xia, S. Murakami, T.M. Nakano, L. Shi, H.Z. Wang, *Wear* 262 (2007) 765.
- [13] P. Bonhote, A. Dias, N. Papageorgiou, K. Kalyanasundaram, M. Gratzel, *Inorg. Chem.* 35 (1996) 1168.
- [14] J. Qu, J.J. Truhan, S. Dai, H. Luo, P.J. Blau, *Tribol. Lett.* 22 (2006) 207.
- [15] X.Q. Liu, F. Zhou, Y.M. Liang, W.M. Liu, *Wear* 261 (2006) 1174.
- [16] A.E. Jimenez, M.D. Bernudez, F.J. Carrion, G.M. Nicolas, *Wear* 261 (2006) 347.
- [17] W.M. Liu, C.F. Ye, Q.Y. Gong, H.Z. Wang, P. Wang, *Tribol. Lett.* 13 (2002) 81.
- [18] B. Bhushan, A.V. Kulkarni, *Langmuir* 11 (1995) 3189.
- [19] T. Kasai, B. Bhushan, *J. Vac. Sci. Technol. B* 23 (2005) 995.
- [20] K.K. Lee, B. Bhushan, D. Hansford, *J. Vac. Technol. A* 23 (2005) 804.
- [21] S.M. Hsu, *Tribol. Int.* 37 (2004) 553.
- [22] B. Bhushan, X.D. Li, *J. Mater. Res.* 12 (1997) 54.
- [23] Z. Fei, D. Zhao, T.J. Geldbach, R. Scopelliti, P.J. Dyson, *Chem. Eur. J.* 10 (2004) 4886.
- [24] S.L. Ren, S.R. Yang, Y.P. Zhao, T.X. Yu, X.D. Xiao, *Surf. Sci.* 546 (2003) 64.
- [25] S.K. Sinha, M. Kawaguchi, T. Kato, F.E. Kenedy, *Tribol. Int.* 36 (2003) 217.
- [26] X.D. Xiao, J. Hu, D.H. Charych, M. Salmeron, *Langmuir* 12 (1996) 235.
- [27] Y. Bo, F. Zhou, Z.G. Mu, Y.M. Liang, W.M. Liu, *Tribol. Int.* 39 (2006) 879.